Proceedings of 9th IOE Graduate Conference
Peer Reviewed
ISSN: 2350-8914 (Online), 2350-8906 (Print)
Year: 2021 Month: March Volume: 9

Synthesis and Characterizations of Activated Carbon from Bayer (Ziziphus Mauritiana) Seeds and its Possibility in Energy Storage Application

Jeevan Ghimire [a], Manoj Kumar Jha [b], Dinesh Shah [c], Hem Raj Pant [d], Sahira Joshi [e]

[a, b, c, d, e] *Department of Applied Sciences and Chemical Engineering, Pulchowk Campus, IOE, TU, Nepal*
Corresponding Email: [a] rejeevanghimi7@gmail.com, [b] jhamanoj144@gmail.com, [c] jh2dineshshah@gmail.com, [d] hempant@ioe.edu.np, [e] sjoshi61@hotmail.com

Abstract
Activated carbons (ACs) were prepared from Bayer (Ziziphus Mauritiana) seed stone, an agricultural waste found in Nepal, by chemical activation with potassium hydroxide (KOH) in 1:1 ratio by weight at two different temperature (500℃-700℃). Char and activated char were also prepared from this carbon precursor. The physiochemical properties of as-prepared ACs were examined using Iodine number, Methylene Blue number, Field Emission scanning electron microscopy (FE-SEM) and BET surface area analysis. Results showed that the activated carbon prepared at 700℃ has the highest porosity and surface area. Therefore, this highly porous AC was employed as an electrode material to evaluate its possible applicability in energy storage devices. Results showed that the electrochemical performance of this AC in an acidic electrolyte is better than that in neutral electrolyte. Therefore, as-synthesized activated carbon at 700℃ is suitable for adsorbent material and can also be applied for energy storage applications.

Keywords
Activated Carbon, Ziziphus Mauritiana, Microporous Material, Mesoporous Material, Energy Storage

1. Introduction

The population growth and depletion of fossil fuels requires sustainable and renewable energy source. To solve these problems, renewable energy source such as solar, wind, geothermal energy etc. have been developed. The renewable energies need to store electric power in energy storage devices, such as, batteries and supercapacitors that are essential to store and use the harvested energy efficiently. In contrast to batteries and conventional dielectric capacitors, supercapacitors have more advantages, such as, longer cycle life, faster charging-discharging rate and better operation safety over other secondary batteries [1]. Supercapacitors can carry very high power density with the lowest stored energy than batteries. For that reason, supercapacitors are mainly appropriate for applications, where high power is needed within few seconds. Compared to typical capacitors, the large electrode surface area in supercapacitors can produce enormous energy storage ability or high capacitance values (expressed in Farads), because large amount of double layers are formed [2, 3].

One of the most important components of a supercapacitor is the electrode. Usually, conducting polymers, metal oxides, and porous materials, such as, activated carbon, carbon aerogels and carbon nanotubes are used for this purpose [3]. Activated carbon (AC) is widely used as an electrode material in electric double layer capacitor (EDLC), because of its high surface area, better porosity, good thermal and electrical conductivity, high chemical stability, low cost and commercially availability. Activation methods and the precursor materials are the two major factors, which may manipulate the final structure and the cost of ACs. The precursor materials of ACs is inexpensive agricultural by-products such as, Bayer seeds stones, cherry stones, peach stones, vine shoots, spirit lees, coconut shells, bamboos, corncob, candlenut shell, acorn shell, orange peels, banana peels etc. [4, 5, 6, 10].

2. Materials and Methods

Locally available Bayer (Ziziphus Mauritiana) found in terai region of Nepal from local market. Potassium

hydroxide (KOH) from Fisher Scientific, sulphuric acid (H2SO4) from Fisher Scientific, hydrochloric acid (HCl) from Fisher Scientific, sodium thiosulphate (Na2S2O3•5H2O) from Fisher Scientific, potassium dichromate (K2Cr2O7) from Fisher Scientific, potassium iodide (KI) from Fisher Scientific, ultra-high purity nitrogen gas and Commercial activated carbon from Qualigens Fine Chemicals were used as received for this study.

20gm Bayer seed powder and 20gm of activating agent (KOH) were taken in a beaker (1:1 ratio by weight) and was mixed with 40ml of water. Then the mixer was manually stirred by glass rod at 70°C until excess moisture has evaporated in a hot plate. The obtained product was kept in the tubular electric furnace in the middle of quartz glass tube for the carbonization at 500°C and 700°C under the flow of N2 gas (100cc/min) for 3 hours. After carbonization process, the carbonized product was repeatedly washed with warm distilled water until the pH value comes in the range of 7 to 7.5 and the sample was dried in oven at 110°C for about 24 hrs. The dried sample was then sieved to get the particles of size 108 µm. Further characterization process begins after preparation of activated carbon.

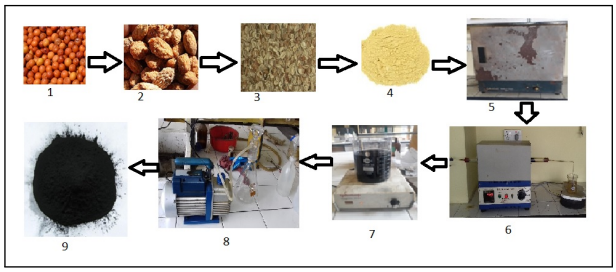

Figure 1: Overall process for the preparation of AC

3. Results and Discussion

3.1 Iodine Number Analysis

The iodine number of different AC was obtained as in adjacent figure 2. The iodine number gives the micro-porosity present in an AC. Higher the iodine number means the higher number of micro-pores present in an AC. The result shows that the KOH AC at 700°c has the highest number of iodine number (938.850 mg/g) which is comparable to that of commercial sample (963.886 mg/g).

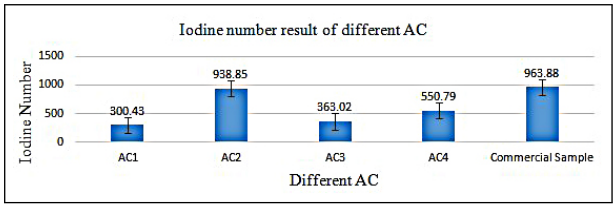

Figure 2: Iodine number result

3.2 Methylyne Blue Number Analysis

The Methylene blue number of different AC was obtained as in adjacent figure 3

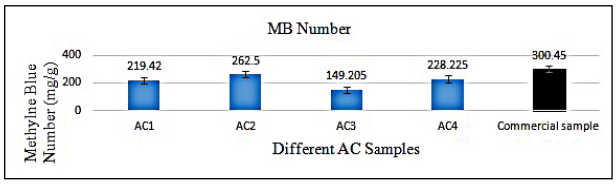

Figure 3: Methylene blue number result

The Methylene blue number gives the mesoporosity present in an AC. Higher the Methylene blue number means the higher number of mesopores present in an AC. The result shows that the KOH AC at 700oc has the highest number of methylene blue number (262.5 mg/g) which is comparable to that of commercial sample (300.45 mg/g).

3.3 Surface Area Analysis

The Surface Area of different AC was given in Table 1.

Table 1: Surface Area result

SN	Activated Carbon	Surface Area (m^2g^{-1})
1	KOH at 500 °C (AC1)	323.821
2	KOH at 700 °C (AC2)	713.063
3	Char at 500 °C (AC3)	331.732
4	Char + KOH at 500 °C (AC4)	447.081
5	Commercial Sample (AC5)	763.976

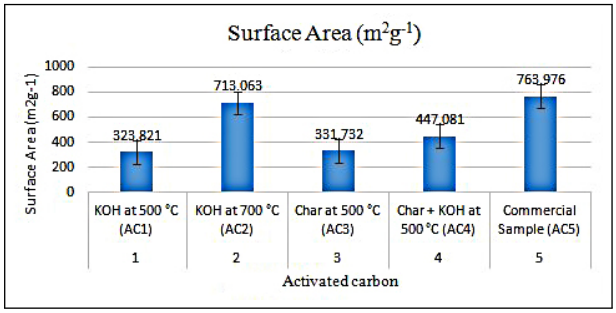

Figure 4: Surface Area Result

Among different samples of activated carbon, the KOH AC at 700°C has the highest surface area (713.063 m2g-1) which is comparable to that of commercial sample (763.976 m2g-1). This surface area was obtained from iodine and methylene blue number, which gives the average area of an activated carbon but precise area of AC was obtained by BET analysis where surface area of KOH activated at 700°C AC sample was found to be 874.56 m2g-1.

3.4 FE-SEM Analysis

The surface morphologies of different sample of activated carbon were investigated using FE-SEM analysis.

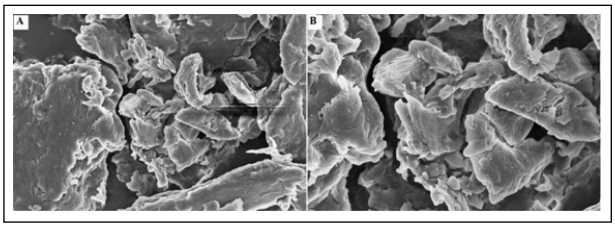

Figure 5: FE-SEM image of Raw sample of Bayer Seed Powder. (A) 10K (B) 20K

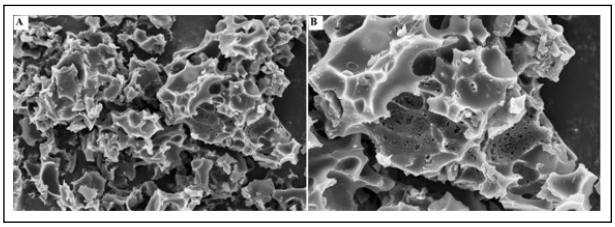

Figure 6: FE-SEM images of KOH AC at 500°C (A) 10K (B) 20K

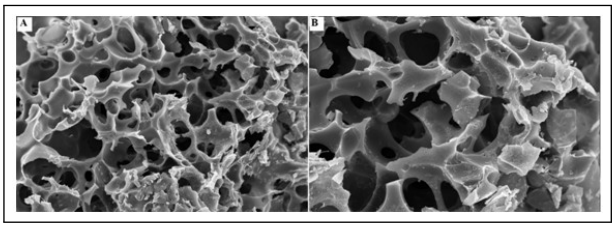

Figure 7: FE-SEM image of KOH AC at 700°C. (A) 10K (B) 20K

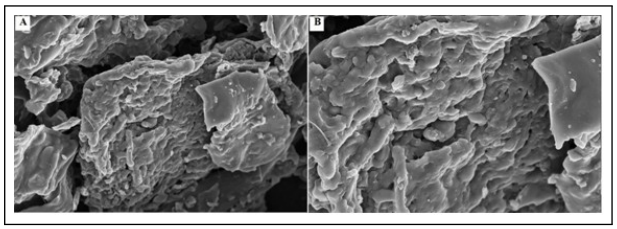

Figure 8: FE-SEM image of Char AC at 500°C. (A) 10K (B) 20K

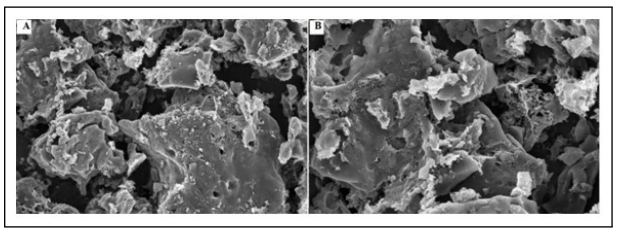

Figure 9: FE-SEM image of Char+KOH AC at 500°C. (A) 10K (B) 20K

The morphological structure of FE-SEM images at 10K and 20K magnification of different sample shows that the raw powder sample of Bayer seed does not contains the well-developed pores on its surface area as in figure 5. However, chemical activation by using potassium hydroxide (KOH) in different temperature on sample, the pores were developed in the activated carbon as in figure 6, 7 and 9. It shows that more porous structure on the surface was seen in the KOH activated carbon at 7000C, however the pores are not uniform in figure 7. Some well-developed and non-uniform porous structure are also seen in KOH activated carbon at 5000C as in figure 6 which is less porous than KOH activated carbon at 7000C. However, in char sample of AC at 500 0C in figure 8, well-developed pores are not seen. These results of FE-SEM images shows that surface area of AC increases if it is chemically activated with KOH at high temperature.

3.5 Nitrogen adsorption–desorption isotherm and pore size distribution graphs

The obtained isotherm was type I, which shows a steep increase in amount of N2 adsorbed with increasing order of relative pressure from 0.1–1 as in figure 10. The microporous structure having the large specific surface area 874.56 m2g-1 (BET surface area) was obtained. The BJH pore size distribution was calculated based on the desorption branch.

Furthermore, the mean pore diameter of the AC was 1.9561 nm, which showed the micropores in AC and total pore volume was 0.42777 cm3g-1 that confirms the microporous surface morphology of FE-SEM result. These results indicated that the action of KOH on crushed carbon precursor followed by heat treatment at high temperature under the inert atmosphere (Nitrogen) leads to the formation of micropores in AC.

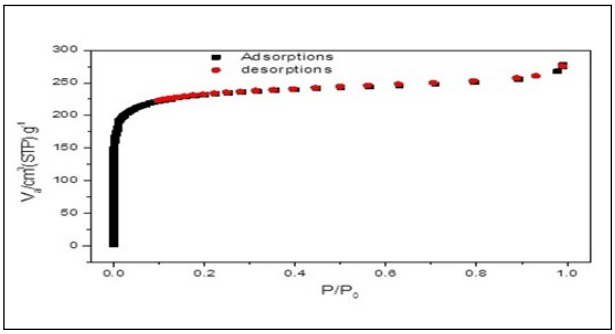

Figure 10: Adsorption Desorption curve of KOH activated at 700°C

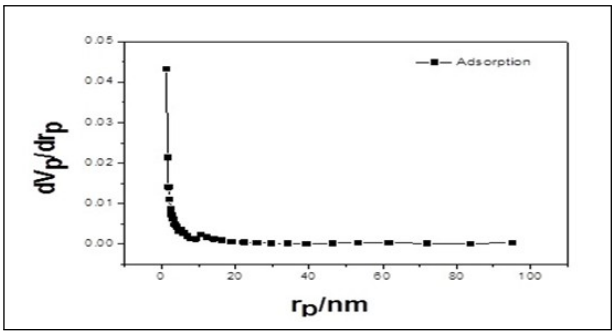

Figure 11: BJH pore size distribution of KOH activated at 700°C

3.6 Electrochemical performance of AC under Acidic and Neutral electrolyte

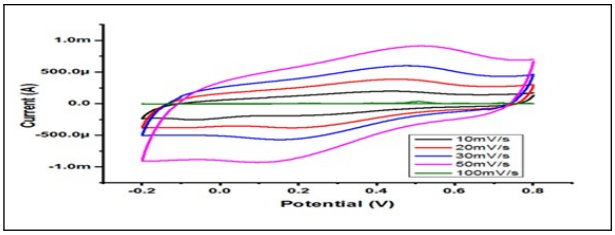

Figure 12: Current potential curve under acidic electrolyte

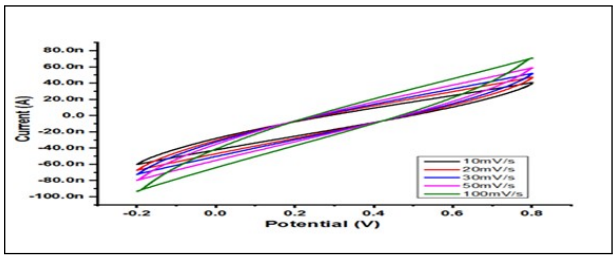

Figure 13: Current potential curve under neutral electrolyte

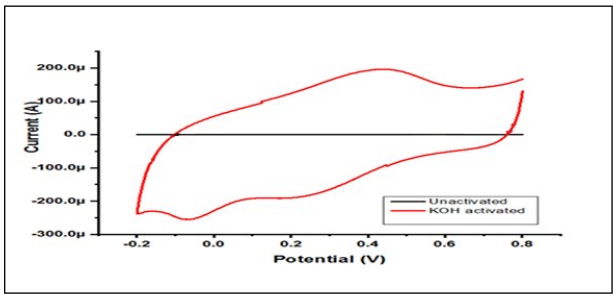

Figure 14: Current potential curve of KOH AC at 700°C and power sample of Bayer seed

The above Fig 12 and 13 shows the electrochemical performance of the AC under the acidic and neutral electrolyte respectively. The CV profile of the AC has demonstrated the ideal rectangular shape at various scan rates as shown in Fig. 12. It indicates that the AC electrode showed the behavior of an electric double layer capacitor (EDLC) in the given potential range [7,8]. The Cyclic Voltammetry (CV) measurement was also conducted at various scan rates under the neutral electrolytes as shown in Fig. 13. The difference between the rectangular shapes of the CV curves with their electrochemical performance under these two electrolytes (acidic and neutral) was obtained by the fast and efficient charge transfer in 1 M H2SO4 [7]. As the loop area of CV curve under acidic medium is larger than that of neutral medium, which shows the good electrochemical performance in acidic medium. Furthermore, the electrochemical performance of Bayer powder sample and KOH AC at 700OC was also measured but powder Bayer sample does not gave effective result as compare to KOH AC from Bayer seed stone at 700OC as the loop area covered by powder sample is very less than that of KOH AC at 7000C which is shown in Fig. 14.

3.7 Galvanostatic Charge-Discharge curve (GCD)

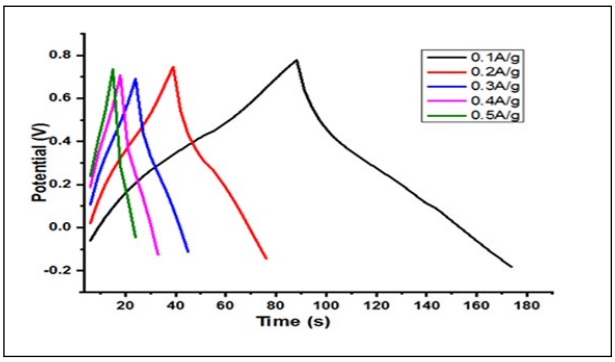

Figure 15: Charge Discharge curve of KOH treated AC at 700°C under acidic electrolyte

The average specific capacitances of the AC electrode under the given electrolytes were calculated by the charge/discharge curves using the given equation.

$$Cs = I.Dt/m.DV \quad (1)$$

where, Cs is the specific capacitance (Fg-1), I is the charge-discharge current (A), Dt is the discharge time (s), m is the mass of the active material (g) and DV is the potential window of the working electrode (V).

The Fig. 15 shows that the galvanostatic charge-discharge (GCD) curves of the AC at various current densities from 0.1-0.5 Ag-1 under acidic electrolyte within same potential. All of the GCD curves were identical symmetrical triangular shapes with the excellent linear voltage-time relationship, demonstrating excellent electric double layer capacitive behaviors with fast charge/discharge properties. Moreover, the parallel curves of the discharge components confirmed the AC electrodes work well within the broad potential [9,11]. The symmetrical curves with lower charge/discharge time indicated the internal resistivity of the electrolytes with lower ion mobility between AC electrode and electrolyte within the electrochemical cell. The specific capacitance of AC electrode was found to be 110 Fg-1 at a current density of 0.5Ag-1 under acidic electrolyte. The specific capacitance was obtained using H2SO4 electrolyte due to the smaller size of hydrated H+ ions. The specific capacitance value of the AC electrode was decreased with increasing the current densities (0.5–5 mVs-1) for acidic electrolytes due to the kinetic resistance and insufficient charge transfer onto or across the electrode/electrolyte interface [9]. The cyclic stability of the AC electrode was carried out under acidic electrolyte by cyclic voltammetry method at high scan rate 100 mVs-1 for 1000 cycles. The capacitive retention of AC was significantly increased with the cycling up to 123 percent of the initial cycle at about 400 cycles for acidic electrolyte, and then gradually stable. Therefore, the capacitive retentions of AC for acidic electrolyte was increased during the first few hundred cycles. This could be explained by the facts that most of the electrochemical active sites of AC were easily exposed along the porous surface, subsurface, and deep inside the particles [12]. As the charging and discharging time of supercapacitor is nearly same so it is not sufficient for supercapacitor. If the AC is further modified by, making it more conducting it will be possible to use as an electrode material for supercapacitor.

4. Conclusion

Here, we synthesized a low-cost AC from Bayer seeds stone by chemical activation method. The obtained AC material having a microporous surface with large surface area showed an improved electrochemical performance in an acidic electrolyte compared to a neutral electrolyte at different current densities. Furthermore, the AC electrode obtained trust worthy cyclic stability after 400 cycles for acidic electrolyte. However, Galvanostatic Charge-Discharge curve at different current densities (0.1-0.5 Ag-1) shows the charging and discharging time nearly equal which is not sufficient for supercapacitor for energy storage. If the AC is modified by, making it more conducting it will be possible for the supercapacitor for energy storage application. This work also provides a facile synthesis method to prepare AC materials and pathway for the exploration of other porous carbon-based materials using the waste biomass into high valuable commercial products. This research work only covers the preparation of activated carbon and its possible application in energy storage. The research conducted has been done so far using the minimum resources available in the laboratory. Followings are the recommendations of this research work:

1. Future research is needed during preparation of AC using other activating agent (not only KOH).
2. Preparation of AC at wide range of temperature and further research work on different samples for possible application.

3. Comparison of AC prepared from chemical activation and physical activation method.

4. The cost estimation should be carried out to evaluate the potential application of this AC for electrode material in energy storage and adsorbent material for industrial production.

5. Future research is needed to make AC more conducting so that high performance energy storage devices manufactured.

Acknowledgments

The authors are grateful to Nanomaterials Lab, Department of Applied Sciences and Chemical Engineering, Pulchowk Campus and The World Academy of Science, Trieste, Italy (TWAS) $(project number; 18 - 168RG/CHE/AS_G)$ for supporting this research work.

References

[1] Qaisar Abbas, Mojtaba Mirzaeian, Abraham A. Ogwu, Michal Mazur, and Des Gibson. Effect of physical activation/surface functional groups on wettability and electrochemical performance of carbon/activated carbon aerogels based electrode materials for electrochemical capacitors. *International Journal of Hydrogen Energy*, 45(25):13586–13595, May 2020.

[2] Surya Prasad Adhikari, Ganesh Prasad Awasthi, Kyung-Suk Kim, Chan Hee Park, and Cheol Sang Kim. Synthesis of three-dimensional mesoporous cu–al layered double hydroxide/g-c3n4 nanocomposites on ni-foam for enhanced supercapacitors with excellent long-term cycling stability. *Dalton Trans.*, 47:4455–4466, 2018.

[3] N.H. Basri, M. Deraman, S. Kanwal, I.A. Talib, J.G. Manjunatha, A.A. Aziz, and R. Farma. Supercapacitors using binderless composite monolith electrodes from carbon nanotubes and pre-carbonized biomass residues. *Biomass and Bioenergy*, 59:370–379, 2013.

[4] Youliang Cheng, Linlin Wu, Changqing Fang, Tiehu Li, Jing Chen, Mannan Yang, and Qingling Zhang. Synthesis of porous carbon materials derived from laminaria japonica via simple carbonization and activation for supercapacitors. *Journal of Materials Research and Technology*, 9(3):3261–3271, 2020.

[5] R. Farma, M. Deraman, A. Awitdrus, I.A. Talib, E. Taer, N.H. Basri, J.G. Manjunatha, M.M. Ishak, B.N.M. Dollah, and S.A. Hashmi. Preparation of highly porous binderless activated carbon electrodes from fibres of oil palm empty fruit bunches for application in supercapacitors. *Bioresource Technology*, 132:254–261, 2013.

[6] Priyanka Shrestha, Manoj Kumar Jha, Jeevan Ghimire, Agni Raj Koirala, Rajeshwar Man Shrestha, Ram Kumar Sharma, Bishweshwar Pant, Mira Park, and Hem Raj Pant. Decoration of zinc oxide nanorods into the surface of activated carbon obtained from agricultural waste for effective removal of methylene blue dye. *Materials*, 13(24), 2020.

[7] Jian Tan, Yulai Han, Liang He, Yixiao Dong, Xu Xu, Dongna Liu, Haowu Yan, Qiang Yu, Congyun Huang, and Liqiang Mai. In situ nitrogen-doped mesoporous carbon nanofibers as flexible freestanding electrodes for high-performance supercapacitors. *J. Mater. Chem. A*, 5:23620–23627, 2017.

[8] Hengxing Ji, Zhenhua Qiao Xin Zhao, Yanwu Zhu Jeil Jung, Li Li Zhang Yalin Lu, and Rodney S. Ruoff Allan H. MacDonald. Capacitance of carbon-based electrical double-layer capacitors. *Nature Communications*, February 2014.

[9] Owusu KA, Li J Qu L, Zhao K Wang Z, Hercule KM Yang C, Shi C Lin C, Zhou L Wei Q, and Mai L. Low-crystalline iron oxide hydroxide nanoparticle anode for high-performance supercapacitors. March 2017.

[10] Min Song, Baosheng Jin, Rui Xiao, Li Yang, Yimin Wu, Zhaoping Zhong, and Yaji Huang. The comparison of two activation techniques to prepare activated carbon from corn cob. *Biomass and Bioenergy*, 48:250–256, 2013.

[11] Viet Hung Pham, Thuy-Duong Nguyen-Phan, Xiao Tong, Balasubramaniyan Rajagopalan, Jin Suk Chung, and James H. Dickerson. Hydrogenated tio2@reduced graphene oxide sandwich-like nanosheets for high voltage supercapacitor applications. *Carbon*, 126:135–144, 2018.

[12] Yan J, Wei T Wang Q, Zhang M Jiang L, and Fan Z Jing X. Template-assisted low temperature synthesis of functionalized graphene for ultrahigh volumetric performance supercapacitors. 8(5):4720–4729, May 2014.